Hindawi
Journal of Chemistry
Volume 2022, Article ID 7086057, 11 pages
https://doi.org/10.1155/2022/7086057

Research Article

Solid-Liquid Phase Equilibria of the Quaternary System ($LiCl + LiBO_2 + Li_2B_4O_7 + H_2O$) at 308.15 K: Experimental and Theoretical Prediction

Hongya Shen,[1] Qi Liu,[1] Xiuxiu Yang,[1] Yafei Guo,[1] Dan Li,[2] Lingzong Meng,[2] and Tianlong Deng[1]

[1]*Key Laboratory of Marine Resource Chemistry and Food Technology (TUST), Ministry of Education, College of Chemical Engineering and Materials Science, Tianjin University of Science and Technology, Tianjin 300457, China*
[2]*School of Chemistry and Chemical Engineering, Linyi University, Linyi 276000, China*

Correspondence should be addressed to Yafei Guo; guoyafei@tust.edu.cn and Tianlong Deng; tldeng@tust.edu.cn

Received 13 August 2022; Revised 22 September 2022; Accepted 30 September 2022; Published 11 October 2022

Academic Editor: Hua-Bing Li

The isothermal dissolution equilibrium method was employed to obtain the solubilities and physicochemical properties of the quaternary system ($LiCl + LiBO_2 + Li_2B_4O_7 + H_2O$) at 308.15 K in this work. The dry-salt phase diagram, water-phase diagram, and physicochemical properties, including density, refractive index, and pH against composition in the quaternary system, were established for the first time. The dry-salt phase diagram includes two invariant points, five univariate solubility curves, and four single salt crystalline phase regions ($LiCl{\cdot}H_2O$, $LiBO_2{\cdot}2H_2O$, $LiBO_2{\cdot}8H_2O$ and $Li_2B_4O_7{\cdot}3H_2O$), respectively. In addition, the physicochemical properties of density, refractive index, and pH in the system change regularly with the changing of the lithium metaborate concentration. Based on the Pitzer model, the mixing ion parameters of $\theta_{Cl,B4O5(OH)4}$, $\theta_{B(OH)4,B4O5(OH)4}$ and $\Psi_{(Li,Cl,B4O5(OH)4}$, $\Psi_{Li,B\ (OH)4,B4O5(OH)4}$ and the predictive solubilities in the quaternary system were fitted. Although there is a slight deviation between the calculated and experimental values, the solubility of boron in the quaternary system agrees well, which provides data support for the study of the solubility of boron.

1. Introduction

Qinghai Salt Lake is rich in lithium and boron resources, which have high mining value [1]. After the brine evaporates, a large amount of NaCl and KCl are precipitated [2], and the composition of brine can be regarded as a complex brine system (Li^+, Mg^{2+}//Cl^-, SO_4^{2-}, Borate–H_2O) [3]. The exploitation of lithium from brine resources has become a hot research spot [4, 5]. Since boron in brine is usually borate, it also changes correspondingly with the difference in pH value, coexisting ions, and solution concentration [6]. Therefore, studying the phase equilibria of brine systems with different forms of lithium boron components, especially the deep processing of lithium borate resources, has important strategic significance for the development and utilization of salt lake resources to create high-value-added products and realize the diversification of salt lake products [7–9].

In recent years, owing to the existence of various forms of borate in solution, extensive literature reports have been done on the phase equilibria of boron-containing complex brine systems at different temperatures, for example, ($KBO_2 + K_2SO_4 + H_2O$) system at 288.15 and 308.15 K [10], ($Li_2SO_4 + LiBO_2 + Li_2B_4O_7 + H_2O$) system at 288.15 K [11], ($Li_2B_4O_7 + K_2B_4O_7 + RbB_5O_8 + H_2O$) system at 323 K [12], ($LiCl + LiB_5O_8 + H_2O$) and ($Li_2SO_4 + LiB_5O_8 + H_2O$) systems at 298.15 K [13]. The temperature in the Qinghai salt lake region can reach 308.15 K in summer [14]. Therefore, the phase equilibria study of this brine system has a certain theoretical reference value for the rational development of salt lake resources with solar ponds technology. Although some subsystems such as ($LiCl + LiBO_2 + H_2O$) at 288.15,

Table 1: Relevant reagents used in this work.

Chemical name	CAS reg. NO.	Grade	Initial mass fraction purity	Purification method	Final mass fraction purity	Analysis method
[a]$LiCl{\cdot}H_2O$	10102-25-7	AR.	0.99	Recrystallization	0.992	Titration for Cl^-
[b]$LiBO_2{\cdot}8H_2O$	63454-43-3	AR.	0.99	Recrystallization	0.992	Titration for BO_2^-
[c]$Li_2B_4O_7$	12007-60-2	AR.	0.99	Recrystallization	0.992	Titration for $B_4O_7^{2-}$

[a]AR from Shanghai Macklin Biochemical Technology Co., Ltd. [b]AR from Sinopharm Chemical Reagent Co., Ltd. [c]AR from Sinopharm Chemical Reagent Co., Ltd.

298.15, 308.15 K and 323.15 K [15–17] and ($LiBO_2 + Li_2B_4O_7 + H_2O$) at 288.15, 298.15 and 323.15 K [11, 18] have been reported, the phase equilibrium of the quaternary system ($LiCl + LiBO_2 + Li_2B_4O_7 + H_2O$) has not been reported in the literature. On the other hand, the Pitzer model based on binary and ternary systems has been widely used to calculate the theoretical solubility of salt–water systems [18–20]. Unfortunately, the literature did not report several ion-interaction parameters for the system ($LiCl + LiBO_2 + Li_2B_4O_7 + H_2O$). Therefore, this paper not only presents the solubility and physicochemical properties of the system ($LiCl + LiBO_2 + Li_2B_4O_7 + H_2O$) at 308.15 K but also presents a predictive calculation of the solubility after obtaining the mixing ion-interaction parameters using the Pitzer model.

2. Experimental

2.1. Apparatus and Materials. It can be seen from Table 1 that the purity of the reagents used in this experiment was analytically pure. During this work, deionized distilled water (DDW) was used to prepare a series of artificially synthesized brines and chemical analyses, with conductivity (κ) less than or equal to 1.2×10^{-4} S·m^{-1}.

The solution reached solid-liquid equilibrium by the constant temperature magnetic stirring thermostat (HXC-500-6A, Beijing Fortune Joy Sci. Technology. Co., Ltd.) with a measurement accuracy of 0.1 K. The densities of solution and water were measured by a densitometer (DMA 4500, Anton Paar, Austria) with a measurement accuracy of 0.5 mg·cm^{-3}, and the refractive index (n_D) was measured using an Abbe refractometer (Abbemat 550, Shanghai Trading Co., Ltd.) having an instrument deviation of 0.0003. A high sensitivity pH meter (PH-7310, WTW Co., Ltd. Germany) accurately measured pH values with an error of ±0.001. X-ray powder diffraction with a scan rate of 400°·min^{-1} and a test range of 10–80° (Smartlab, Rigaku, Japan) is used to identify the solid phases. In this work, all experimental data was measured in triplicate and the average was chosen.

2.2. Experimental Methods. After checking the solubility data of the common saturation point of the subsystem in this system, the third salt was mixed in a series of Teflon bottles with a volume of 250 cm^3 from the common saturation point of the ternary system with a certain gradient by isothermal solution equilibrium method. LiCl with mass gradient and the quantitative water were added from the common saturation point of $LiBO_2{\cdot}8H_2O$ and $Li_2B_4O_7{\cdot}3H_2O$ to form a complex. It was put into a constant temperature water bath magnetic stirring tank. The water bath temperature was controlled at (308.15 ± 1) K. Set the stirring speed at 200 rpm to accelerate the formation of the equilibrium. After continuous stirring for about 50 days, when the liquid and solid phases were separated, an appropriate amount of sample was subsequently taken with a clean pipette for analysis. After the remaining samples were continuously stirred for about 60 days, an aliquot of the supernatant solution was taken for reanalysis. When the relative error of the analytical results for the sampling of different solutions (the concentrations of Li^+, Cl^-, BO_2^- and $B_4O_7^{2-}$) was within 0.003 [21], it proved that the brine reached equilibrium. Subsequently, the physicochemical properties of the liquid phase were analyzed by refractive index, density, and pH, corresponding to those of the solid phase studied by X-ray powder diffraction, respectively.

2.3. Analytical Methods. For the quaternary system ($LiCl + LiBO_2 + Li_2B_4O_7 + H_2O$), the mercury titration method was used to measure the concentration of chloride ions with diphenylazocarbazide and bromophenol blue as indicators, and the error of the measurement value was less than 0.003 in a mass fraction [22]. The content of boron was analyzed by a modified mannitol titration with a relative uncertainty of ±0.0005 and recorded as a mass fraction [22]. And the lithium-ion concentration in the solution was measured by ICP-OES (Prodigy, Teledyne Leeman Labs, USA) [11]. Due to the diverse existence of boron in aqueous solutions [6], only the total boron concentration can be measured. However, lithium metaborate and lithium tetraborate as the initial reagents are also the solid equilibrium phases in this experiment. Therefore, we assume that only $B(OH)_4^-$ and $B_4O_5(OH)_4^{2-}$ are present in the solution to measure solubility. Combining the concentrations of lithium and boron, the concentrations of two borates $LiBO_2$ and $Li_2B_4O_7$ are calculated with Eqs. (1) and (2).

$$x + 2y = n_{Li} - n_{LiCl}, \quad (1)$$

$$x + 4y = n_B, \quad (2)$$

where x, y and n_{LiCl} are the molar concentrations of $LiBO_2$, $Li_2B_4O_7$ and LiCl, respectively, and n_{Li} is the total molar concentration of Li^+ in the system. Similarly, n_B is boron (BO_2^-, $B_4O_7^{2-}$) ions of the total molar concentration. Considering the influence of reagent impurity, temperature fluctuation and concentration measurement errors, the standard uncertainty of LiCl concentration was less than 0.003. The uncertainty of $LiBO_2$ and $Li_2B_4O_7$ concentrations did not exceed 0.005.

Table 2: Solubilities in the quaternary system $LiCl - LiBO_2 - Li_2B_4O_7 - H_2O$ at 308.15 K and 0.1 MPa.[a]

No.	Composition of the liquid phase, $100w$[b]			Composition of the liquid phase, $100Z$/[(g/100 g of salt)]				Solid phase[d]
	LiCl	$LiBO_2$	$Li_2B_4O_7$	Z (LiCl)	Z ($LiBO_2$)	Z ($Li_2B_4O_7$)	Z (H_2O)	
1, A[e]	44.25	8.25	0.00	84.29	15.71	0.00	90.48	LC + LB2
2	44.11	7.47	0.12	85.32	14.45	0.23	93.42	LC + LB2
3	43.58	7.06	0.20	85.72	13.89	0.39	96.70	LC + LB2
4, B[e]	3.74	5.18	0.00	41.93	58.07	0.00	1021.08	LB2 + LB8
5	3.65	4.43	0.12	44.51	54.03	1.46	1119.51	LB2 + LB8
6	3.56	4.09	0.17	45.53	52.30	2.17	1178.77	LB2 + LB8
7, C	46.66	0.00	0.21	99.55	0.00	0.45	113.36	LC + LB4
8	45.70	1.43	0.23	96.49	3.02	0.49	111.15	LC + LB4
9	44.94	3.09	0.22	93.14	6.40	0.46	107.25	LC + LB4
10	44.35	4.95	0.24	89.52	9.99	0.49	101.86	LC + LB4
11, F_1	43.69	6.44	0.25	86.29	13.22	0.49	97.51	LC + LB4 + LB2
12	24.86	5.97	0.24	80.01	19.22	0.77	221.85	LB4 + LB2
13	15.07	5.49	0.23	72.48	26.41	1.11	381.00	LB4 + LB2
14	9.58	4.99	0.24	64.69	33.69	1.62	575.22	LB4 + LB2
15	6.62	4.37	0.25	58.90	38.88	2.22	789.68	LB4 + LB2
16, F_2	3.36	3.87	0.26	44.86	51.67	3.47	1235.11	LB4 + LB2 + LB8
17	2.33	3.97	0.28	35.41	60.33	4.26	1419.76	LB4 + LB8
18	1.41	4.66	0.35	21.96	72.59	5.45	1457.63	LB4 + LB8
19, D[e]	0.00	6.18	0.45	0.00	93.21	6.79	1408.30	LB4 + LB8

[a]Standard uncertainties u, $u(T) = 0.02$ K, $u(p) = 0.005$ MPa, u (LiCl) = 0.003, u ($LiBO_2$) = 0.005, and u ($Li_2B_4O_7$) = 0.005. [b]w, mass fraction. [c]Z = Jänecke index. [d]LC: $LiCl{\cdot}H_2O$; LB8: $LiBO_2{\cdot}8H_2O$; LB4: $Li_2B_4O_7{\cdot}3H_2O$; LB2: $LiBO_2{\cdot}2H_2O$. [e]The solubilities were cited from ref. [16, 18].

3. Results and Discussion

3.1. Phase Diagram of the Quaternary System ($LiCl + LiBO_2 + Li_2B_4O_7 + H_2O$). Table 2 shows the solubility of the liquid equilibrium phase in the quaternary system ($LiCl + LiBO_2 + Li_2B_4O_7 + H_2O$) at 308.15 K, where the Jänecke dry-salt index (Zi) is calculated from the mass fraction (w) using equations (3)–(6). Z (B) is calculated based on 100 g of total dry salt, and the specific calculation method is shown in the following formula [22].

$$Z(\mathrm{LiCl}) = \frac{w(\mathrm{LiCl})}{w(\mathrm{LiCl}) + w(\mathrm{LiBO_2}) + w(\mathrm{Li_2B_4O_7})}, \quad (3)$$

$$Z(\mathrm{LiBO_2}) = \frac{w(\mathrm{LiBO_2})}{w(\mathrm{LiCl}) + w(\mathrm{LiBO_2}) + w(\mathrm{Li_2B_4O_7})}, \quad (4)$$

$$Z(\mathrm{Li_2B_4O_7}) = \frac{w(\mathrm{Li_2B_4O_7})}{w(\mathrm{LiCl}) + w(\mathrm{LiBO_2}) + w(\mathrm{Li_2B_4O_7})}, \quad (5)$$

$$Z(\mathrm{H_2O}) = \frac{w(\mathrm{H_2O})}{w(\mathrm{LiCl}) + w(\mathrm{LiBO_2}) + w(\mathrm{Li_2B_4O_7})}. \quad (6)$$

The boundary points A, B, C and D on the dry basis diagram of the quaternary system are the saturation points of the three ternary subsystems ($LiCl + LiBO_2 + H_2O$), ($LiCl + Li_2B_4O_7 + H_2O$) and ($LiBO_2 + Li_2B_4O_7 + H_2O$) shown in Figure 1(a). The dry-salt phase diagram in Figure 1 includes two invariant points F_1 saturated with $LiCl{\cdot}H_2O$, $LiBO_2{\cdot}2H_2O$ and $Li_2B_4O_7{\cdot}3H_2O$ and F_2 saturated with $LiBO_2{\cdot}8H_2O$, $LiBO_2{\cdot}2H_2O$ and $Li_2B_4O_7{\cdot}3H_2O$, five univariant solubility curves corresponding to F_1A ($LiCl{\cdot}H_2O + LiBO_2{\cdot}2H_2O$), CF_1 ($LiCl{\cdot}H_2O + Li_2B_4O_7{\cdot}3H_2O$), F_1F_2 ($LiBO_2{\cdot}2H_2O + Li_2B_4O_7{\cdot}3H_2O$), BF_2 ($LiBO_2{\cdot}2H_2O + LiBO_2{\cdot}8H_2O$), F_2D ($LiBO_2{\cdot}8H_2O + Li_2B_4O_7{\cdot}3H_2O$), and four crystallization fields corresponding to single salts $LiCl{\cdot}H_2O$, $LiBO_2{\cdot}2H_2O$, $LiBO_2{\cdot}8H_2O$, and $Li_2B_4O_7{\cdot}3H_2O$. The size of the crystallization area decreases in the order $Li_2B_4O_7{\cdot}3H_2O$, $LiBO_2{\cdot}2H_2O$, $LiBO_2{\cdot}8H_2O$, and $LiCl{\cdot}H_2O$. The results show that $Li_2B_4O_7{\cdot}3H_2O$ has the smallest solubility and is easy to crystallize from brine. Figure 1(b) is a partial enlargement of the phase diagram in the quaternary system ($LiCl + LiBO_2 + Li_2B_4O_7 + H2O$). Figure 2shows the X-ray diffraction patterns of the invariant points F_1 and F_2. Comparing with the characteristic peaks of the standard PDF card, it shows that the salts $LiCl{\cdot}H_2O + LiBO_2{\cdot}2H_2O + Li_2B_4O_7{\cdot}3H_2O$ and $LiBO_2{\cdot}2H_2O + LiBO_2{\cdot}8H_2O + Li_2B_4O_7{\cdot}3H_2O$ coexist at the invariant points F_1 and F_2.

Figure 3 plots the water content diagram with $Z(LiBO_2)$ and $Z(H_2O)$ as the abscissa and ordinate. In the univariant solubility curve CA, $Z(H_2O)$ has not significantly changed from 113.36 to 90.48. The $Z(H_2O)$ in the univariate solubility curve F_2B decreases with the increase of $Z(LiBO_2)$. The $100Z$ (H_2O) in the curves F_1F_2 and F_2D increases as $100Z$ ($LiBO_2$) increases, reaching the maximum value of 1471.67 at point D. The $100Z$ (H_2O) is 97.51 and 1235.11 at the invariant points F_1 and F_2. In general, the concentration of the solution can be judged by the changing trend of the univariant curves.

3.2. Physicochemical Properties. The relevant physicochemical properties of the electrolyte solution in the quaternary system (LiCl + LiBO2 + Li2B4O7 + H2O), such as density, refractive index and pH value, are shown in Table 3. Figure 4 reflects the variation trend of the physicochemical

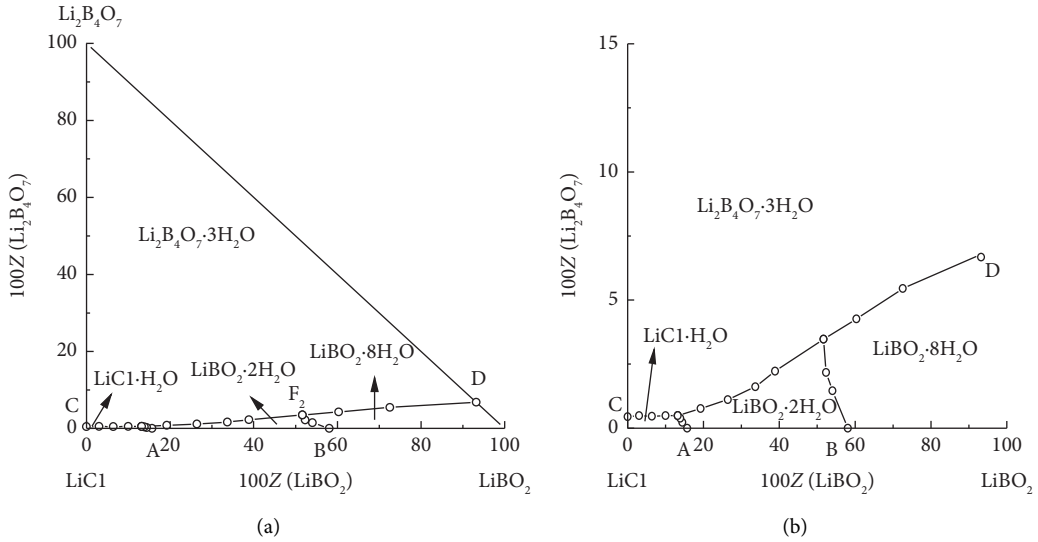

Figure 1: Dry-salt phase diagram of the quaternary system $LiCl - LiBO_2 - Li_2B_4O_7 - H_2O$ at 308.15 K (a) phase diagram; (b) part-enlargement diagram.

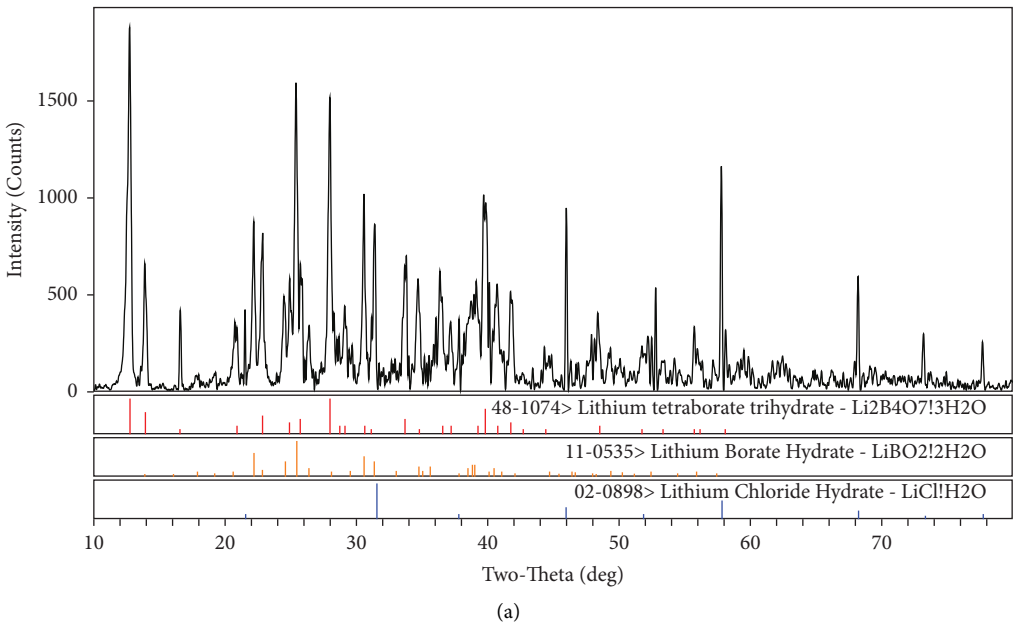

(a)

Figure 2: Continued.

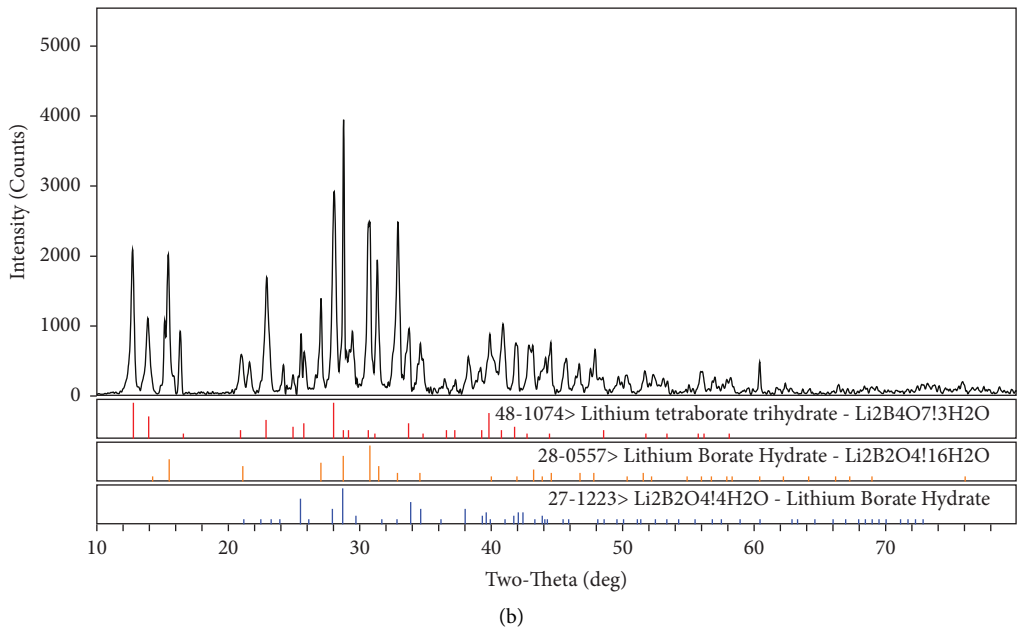

(b)

Figure 2: XRD patterns of the invariant point F1 (a) and F2 (b) in the quaternary system LiCl – $LiBO_2$ – $Li_2B_4O_7$ – H_2O at 308.15 K. (a) $Li_2B_4O_7{\cdot}3H_2O$ + $LiBO_2{\cdot}2H_2O$ + $LiCl{\cdot}H_2O$. (b) $Li_2B_4O_7{\cdot}3H_2O$ + $LiBO_2{\cdot}2H_2O$ + $LiBO_2{\cdot}8H_2O$.

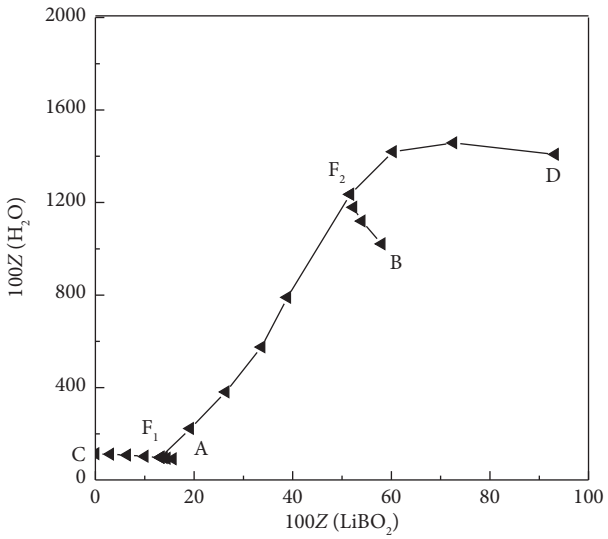

Figure 3: Water content diagram of the quaternary system LiCl – $LiBO_2$ – $Li_2B_4O_7$ – H_2O at 308.15 K.

properties in this system with $Z(LiBO_2)$. The change rule of densities in Figure 4(a) is roughly consistent with the refractive indices in Figure 4(b). As Z(LiBO2) increases, the values also increase in the curves of CF1 and F1A, reaching their maximum (1.3846 g·cm−3 and 1.4594) at point A. But values sharply decrease in the curves of F1F2, and there are minimums (1.0633 and 1.3454) at point F2. Moreover, the changing trend of the pH curve in Figure 4(c) is different from that of the former two. The pH value in the liquid phase gradually increases from point C (4.14) to point D (10.65). The specific trend of the pH value increases from C to F2 and decreases in the F1A and F2B curves with the increase of $Z(LiBO_2)$. The densities, refractive indices, and pH values in the curve of F2D have almost the same trend.

Calculate density (ρ) and refractive index (n_D) from reported empirical equations [23].

$$\ln \frac{n_D}{n_{D0}} = \sum B_i w_i,$$
$$\ln \frac{\rho}{\rho_0} = \sum A_i w_i. \quad (7)$$

In the above formula, ρ and n_D are the density values and the refractive indices in the solution. Correspondingly, ρ_0 and n_{D0} represent pure water at 308.15 K, while ρ_0 is 0.99484 g·cm^{-3} and n_{D0} is 1.33131. W_i expressed the mass fraction of the i-th component in the solution. A_i and B_i, denote constants for the i-th component of the density and refractive index in solution, which can be fitted with the experimental data. For LiCl, $LiBO_2$ and $Li_2B_4O_7$, A_i is 0.005466, 0.01083, and 0.02935, and B_i is 0.001574, 0.002357, and 0.003915, respectively. Except for a few complicated points, the difference between the calculated results and the measured densities and refractive index do not exceed 0.0080 and 0.0056, respectively, which proves the reliability of the data.

4. Solubility Prediction

4.1. Model Parameterization. Among many complex thermodynamic calculation models of water-salt systems, the Pitzer model is widely used in the calculation of solubility of water-salt systems [16, 24]. However, at present, there is no literature on thermodynamic calculations based on the

Table 3: Physicochemical properties of the quaternary system $LiCl - LiBO_2 - Li_2B_4O_7 - H_2O$ at 308.15 K and 0.1 MPa.[a]

No.b	ρ/g·cm−3			nD			pH
	Experimental Value	Calculated Value	Relative Error, %	Experimental Value	Calculated Value	Relative Error, %	
1, Ac	1.3846	1.3855	0.07	1.4594	1.4554	−0.28	5.49
2	1.3756	1.3776	0.15	1.4531	1.4531	0.00	5.93
3	1.3703	1.3708	0.04	1.4520	1.4509	−0.08	6.17
4, Bc	1.0718	1.0740	0.20	1.3607	1.3556	−0.37	10.35
5	1.0670	1.0685	0.14	1.3568	1.3537	−0.23	10.42
6	1.0642	1.0656	0.13	1.3548	1.3527	−0.16	10.47
7, C	1.2815	1.2918	0.80	1.4372	1.4339	−0.23	4.14
8	1.3098	1.3059	−0.30	1.4447	1.4367	−0.56	4.89
9	1.3288	1.3237	−0.39	1.4474	1.4406	−0.47	5.51
10	1.3484	1.3470	−0.10	1.4489	1.4457	−0.22	6.12
11, F1	1.3675	1.3644	−0.22	1.4503	1.4493	−0.07	6.25
12	1.2252	1.2244	−0.07	1.4077	1.4054	−0.16	8.39
13	1.1557	1.1542	−0.13	1.3896	1.3823	−0.53	9.15
14	1.1139	1.1144	0.04	1.3636	1.3688	0.38	9.79
15	1.0915	1.0895	−0.19	1.3578	1.3605	0.20	10.32
16, F2	1.0633	1.0647	0.14	1.3454	1.3520	0.49	10.50
17	1.0650	1.0605	−0.42	1.3474	1.3502	0.21	10.55
18	1.0670	1.0653	−0.16	1.3483	1.3509	0.19	10.56
19, D	1.0726	1.0778	0.48	1.3521	1.3532	0.08	10.65

[a] Standard uncertainties u, u (T) = 0.02 K, u (p) = 0.005 MPa, u (ρ) = 0.005 g cm−3. u (nD) = 0.002, u (pH) = 0.01. [b] The no. Column corresponds to the no. Column in Table 2. [c] The physicochemical properties were cited from ref. [16].

Pitzer ionic interaction model for quaternary systems ($LiCl + LiBO_2 + Li_2B_4O_7 + H_2O$). Therefore, we will use the Pitzer model to fit the solubility data of this system at 308.15 K. The primary expressions for calculating solubility in this model are equations (8) to (10) [24].

$$(\Phi - 1) = \left(\frac{2}{\sum_i i) \left[\frac{-A^{\Phi} I^{3/2}}{I + bI^{1/2}} \right] + \sum_c \sum_a m_c m_a \left(B^{\Phi}_{ca} + ZC_{ca} \right) + \sum_c \sum_{<c'} m_c m_{c'} \left(\Phi^{\Phi}_{cc'} + \sum_a m_a \Psi_{cc'a} \right), + \sum_a \sum_{<a'} m_a m_{a'} \left(\Phi^{\Phi}_{aa'} + \sum_c m_c \Psi_{caa'} \right),} \right) \tag{8}$$

$$\ln \gamma_M = Z_M^2 F + \sum_a m_a \left(2B_{Ma} + ZC_{Ma} \right) + \sum_c m_c \left(\Phi_{Mc} + \sum_a m_a \Psi_{Mca} \right) + \sum_a \sum_{<a'} m_a m_{a'} \Psi_{Maa'} + z_M \sum_c \sum_a m_c m_a C_{ca}, \tag{9}$$

$$\ln \gamma_X = Z_M^2 F + \sum_c m_c \left(2B_{cX} + ZC_{cX} \right) + \sum_a m_a \left(\Phi_{Xa} + \sum_c m_c \Psi_{cXa} \right) + \sum_c \sum_{<c'} m_c m_{c'} \Psi_{cc'X} + z_X \sum_c \sum_a m_c m_a C_{ca}, \tag{10}$$

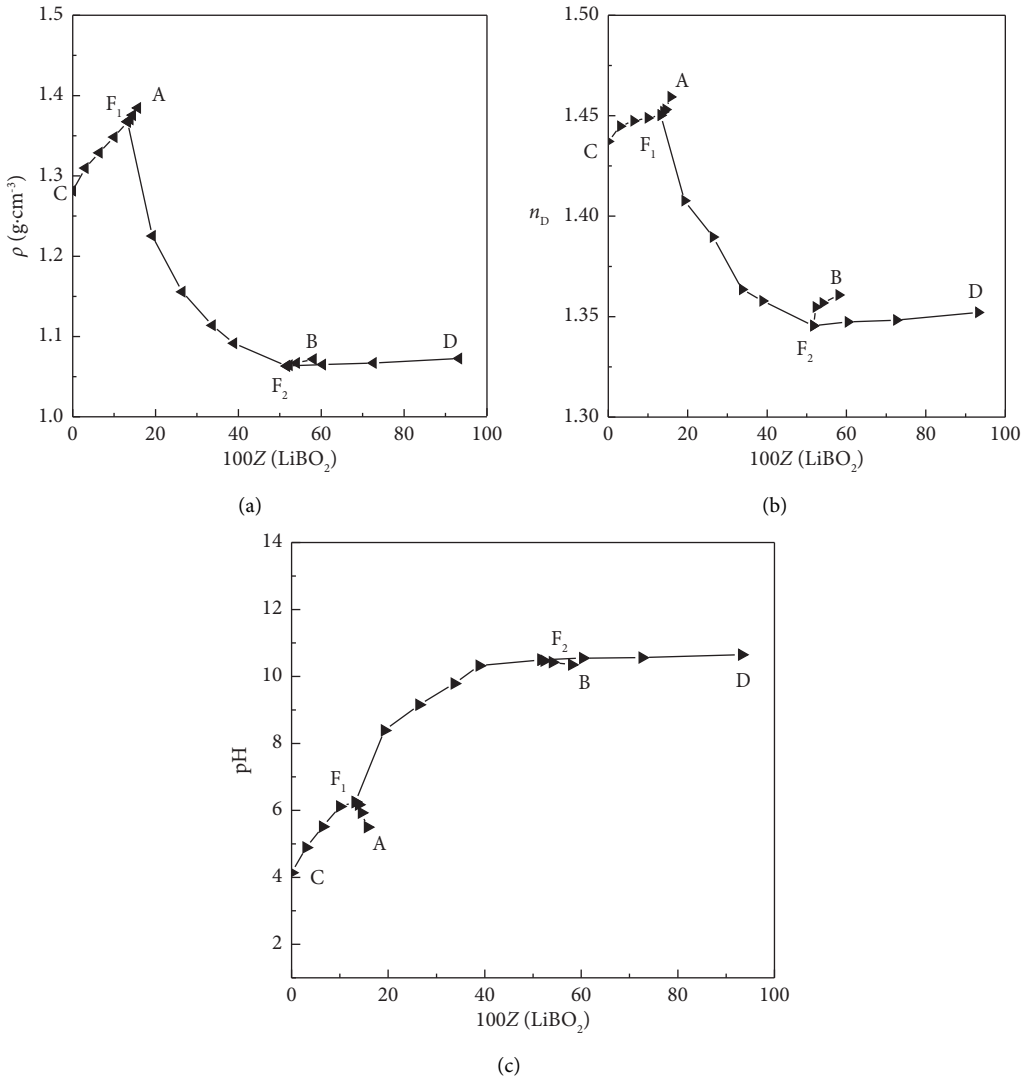

Figure 4: Physicochemical properties versus composition diagram of the quaternary system LiCl – $LiBO_2$ – $Li_2B_4O_7$ – H_2O at 308.15 K (a) density versus 100Z ($LiBO_2$); (b) refractive index versus 100Z ($LiBO_2$); (c) pH versus 100Z ($LiBO_2$).

Table 4: Pitzer single salt parameters of electrolyte in the quaternary system LiCl – $LiBO_2$ – $Li_2B_4O_7$ – H_2O at 308.15 K.

Parameters	α_1	α_2	$\beta^{(0)}$	$\beta^{(1)}$	$\beta^{(2)}$	$C^{(\emptyset)}$	Ref.
LiCl	—	—	0.1469	0.3134		0.003240	[26]
LiCl	2.0	0.0	0.2016	−0.1879	0.0	−0.004044	[12]
LiB $(OH)_4$	1.4	1.5	−0.2706	41.8193	−44.3491	0.007996	[12]
$Li_2B_4O_5$ $(OH)_4$	2.0	0.0	−0.331042	−0.152813	0.0000	0.01012000	[27]

where the subscripts M, c, and c' are the cations in the solution, X, a and a' are the anions in the solution, Z_i represents the valence of the ions, m_i refers to the concentration of the substance in the solution (mol·kg^{-1}), Φ and i are the permeability coefficient and activity coefficient. Other symbols in the equations, for instance, F, C, Z, A^{Φ}, B^{Φ}, and B are described in references [25, 26]. However, Debye–Hückel parameter A^{Φ} at 308.15 K is 0.398535 in the study.

At a specific temperature and pressure, the solubility equilibrium constant (K_{sp}) of the hydrated salt for the dissolution reaction can be obtained by the following formula [24].

$$\begin{aligned} &M_{\nu_M}X_{\nu_X} \cdot nH_2O = \nu_M M^{\nu+} + \nu_X X^{\nu-} + nH_2O, \\ &\ln K_{sp} = \nu_M \ln(m_M\gamma_M) + \nu_X \ln(m_X\gamma_X) + n\ln\alpha_W, \\ &= \nu_M \ln m_M + \nu_M \ln\gamma_M + (\nu_X + \nu_X)\ln\gamma_\pm + n\ln\alpha_W, \end{aligned} \tag{11}$$

where γ_M and γ_X are the activity coefficient, and the mean activity coefficient is denoted by $\gamma_\pm$.

Table 5: Pitzer mixing parameters in the quaternary system $LiCl - LiBO_2 - Li_2B_4O_7 - H_2O$ at 308.15 K.

Species	θ	Ψ	Ref.
Cl^-,$B(OH)_4^-$	−0.1781		[12]
Cl^-,$B_4O_5(OH)_4^{2-}$	−0.1500		This work
$B(OH)_4^-$, $B_4O_5(OH)_4^{2-}$	0.0620		This work
Li^+,Cl^-,$B(OH)_4^-$		0.006856	[12]
Li^+,Cl^- $B_4O_5(OH)_4^{2-}$		0.0233	This work
Li^+,$B(OH)_4^-$, $B_4O_5(OH)_4^{2-}$		0.0000	This work

Table 6: Comparison of experimental and calculated values of invariant points in the quaternary system $LiCl - LiBO_2 - Li_2B_4O_7 - H_2O$ at 308.15 K.[a]

No.[b]	Value	Composition of the liquid phase, $100w$[b]			Equilibrium solid phase
		LiCl	$LiBO_2$	$Li_2B_4O_7$	
C	Experimental	46.66	0.00	0.21	$LiCl{\cdot}H_2O + Li_2B_4O_5(OH)_4{\cdot}H_2O$
Experimental calculated	Calculated	46.66	0.00	0.25	$LiCl{\cdot}H_2O + Li_2B_4O_5(OH)_4{\cdot}H_2O$
Experimental calculated	Experimental	0.00	6.18	0.45	$LiB(OH)_4{\cdot}6H_2O + Li_2B_4O_5(OH)_4{\cdot}H_2O$
C	Calculated	0.00	10.65	0.55	$LiB(OH)_4{\cdot}6H_2O + Li_2B_4O_5(OH)_4{\cdot}H_2O$
D	Experimental	43.69	6.44	0.25	$LiCl{\cdot}H_2O + LiB(OH)_4 + Li_2B_4O_5(OH)_4{\cdot}H_2O$
D	Calculated	43.69	11.10	0.30	$LiCl{\cdot}H_2O + LiB(OH)_4 + Li_2B_4O_5(OH)_43H_2O$
F_1	Experimental	3.36	3.87	0.26	$LiB(OH)_4 + LiB(OH)_4{\cdot}6H_2O + Li_2B_4O_5(OH)_4{\cdot}H_2O$
F_1	Calculated	3.36	6.67	0.32	$LiB(OH)_4 + LiB(OH)_4{\cdot}6H_2O + Li_2B_4O_5(OH)_4{\cdot}H_2O$

[a]Standard uncertainties u, u (T) = 0.02 K, u (p) = 0.005 MPa, u (LiCl) = 0.003, u ($LiBO_2$) = 0.005, and u ($Li_2B_4O_7$) = 0.005. [b]The no. Column corresponds to the no. Column in Table 2.

Boron exists in various forms in borate solution, in which $B(OH)_4^-$ and $B_4O_5(OH)_4^{2-}$ are on behalf of the metaborate and tetraborate ions [6, 27]. In addition, other existing forms of boron lack the relevant Pitzer binary and mixing parameters at 308.15 K, so thermodynamic properties cannot be fitted. Therefore, we only selected $B(OH)_4^-$ and $B_4O_5(OH)_4^{2-}$ two ions for solubility calculations. The single salt parameters of LiCl and $LiB(OH)_4$, and the solubility product constants (*Ksp*) of $LiCl{\cdot}H_2O$, $LiBO_2{\cdot}2H_2O$ and $LiBO_2{\cdot}8H_2O$ were obtained from the literature [16, 28]. The single salt parameters of $Li_2B_4O_5(OH)_4$ at 308.15 K were lacking in the literature, and the temperature is close to 298.15 K, so Deng's parameters at 298.15 K were chosen in the calculation [29]. The Pitzer mixing parameters $\theta_{Cl,B(OH)4}$ and $\varphi_{Li,Cl,B(OH)4}$ were cited from our pervious work [16]. The missing Pitzer mixing parameters $\theta_{Cl,B4O5(OH)4}$ and $\varphi_{Li,Cl,B4O5(OH)4}$ were fitted with the solubilities of the system $LiCl - Li_2B_4O_7 - H_2O$ at 308.15 K [30]. The parameters $\theta_{B(OH)4,B4O5(OH)4}$ and $\varphi_{Li,B(OH)4,\ B4O5(OH)4}$ were reported in our previous [31]. However, the calculated solubility data with above parameters for points F_1 and F_2 show great deviation with the experimental results. The parameters $\theta_{B(OH)4,B4O5(OH)4}$ and $\varphi_{Li,B(OH)4,\ B4O5(OH)4}$ were adjusted again. The single salt parameters and mixing ion parameters of the system used in the study are shown in Tables 4 and 5.

Pitzer mixing parameters $\theta_{Cl,B4O5(OH)4}$, $\theta_{B(OH)4,B4O5(OH)4,}$ $\Psi_{(Li,Cl,B4O5(OH)4}$, and $\Psi_{Li+,B(OH)4,4O5(OH)4}$ mixing parameters in the quaternary system.

4.2. Solubility Calculation. Before using the Pitzer model to calculate the solubility of the system ($LiCl + LiBO_2 + Li_2B_4O_7 + H_2O$) at 308.15 K, it is necessary to obtain the corresponding Pitzer parameters. It can be seen from the existing literature that when $LiCl{\cdot}H_2O$, $LiBO_2{\cdot}2H_2O$, $LiBO_2{\cdot}8H_2O$, and $Li_2B_4O_7{\cdot}3H_2O$ are in the dissolution equilibrium, the solubility product constants (ln*Ksp*) are 12.0072, −1.0200, −0.5140, and −7.5511, respectively [31]. We calculated the solubility at 308.15 K by combining the above $\ln K_{sp}$ values, Pitzer single parameters and the mixing parameters. Table 6 lists the solubilities for the boundary points and invariant points in the quaternary system ($LiCl + LiBO_2 + Li_2B_4O_7 + H_2O$) at 308.15 K, and the corresponding phase diagram is shown in Figure 5. The calculated phase diagram indicated by the red dotted line cannot completely coincide with the experimental data curve. There is an obvious deviation, especially in the solubility curves for $LiBO_2{\cdot}8H_2O$ and $Li_2B_4O_7{\cdot}3H_2O$ saturation. The calculated saturation solubility isotherms for $LiBO_2{\cdot}8H_2O$ and $Li_2B_4O_7{\cdot}3H_2O$ were still significantly inconsistent with the experimental data despite changing the mixing parameters several times. At point C, the experimental value is closest to the calculated value, and the relative error is the smallest. At the invariant points F_1 and F_2, the deviation of lithium borate content are larger, while the deviation of lithium chloride is smaller. Therefore, the solubility calculated by the Pitzer model cannot exactly match the experimental value. However, except for curve DF_2 in Figure 5, the fitted values on other solubility curves are consistent with the experimental data, indicating that the Pitzer model can explain the solubility changes very well.

At the F_1 point, the maximum deviation between the mass fraction of w(LiCl), $w(LiBO_2)$ and $w(Li_2B_4O_7)$ and the theoretical value is 0,0.0466, 0.0005, respectively, and the

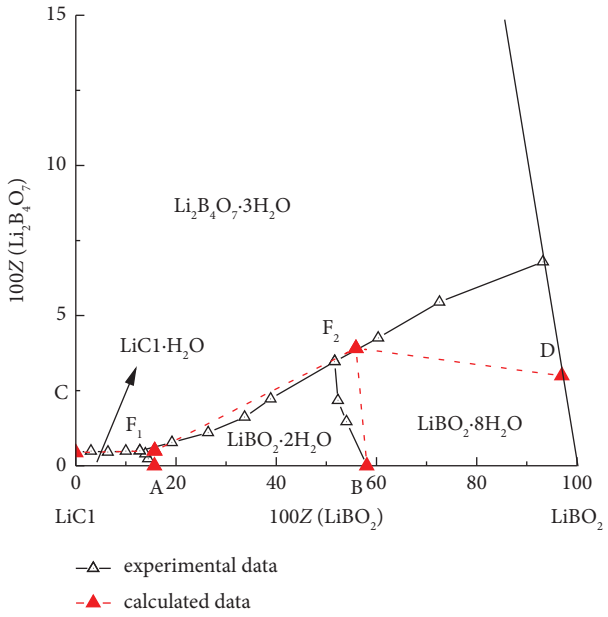

Figure 5: Experimental and calculated phase diagram in quaternary system LiCl – $LiBO_2$ – $Li_2B_4O_7$ – H_2O at 308.15 K; red dashed lines for the calculated data, solid black lines for the experimental data.

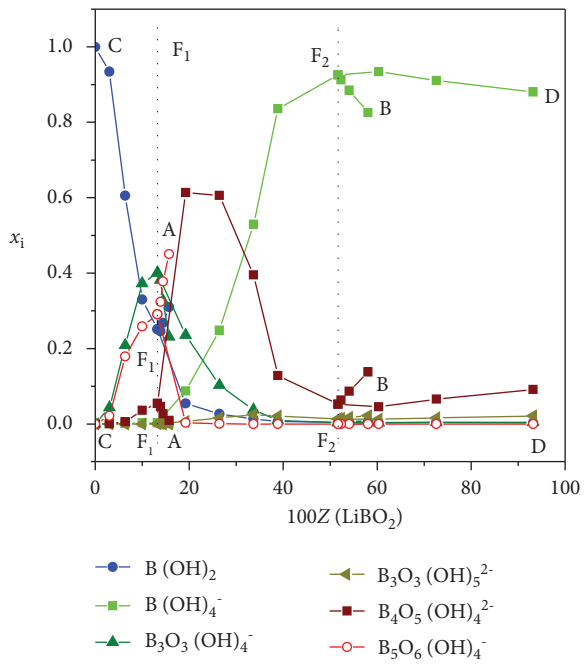

Figure 6: Boron species distribution in solution in the quaternary system LiCl–– $LiBO_2$–– $Li_2B_4O_7$–– H_2O at 308.15 K.

deviation value at the F_2 point is 0,0.028, 0.0006, respectively. However, the variation trend of the solubility curve calculated in Figure 5 is consistent with the experimental results, indicating that the Pitzer model can be used to describe solubility. The error between the experimental value and the calculated value is caused for various reasons. The parameters required in the calculations are derived from different kinds of literature and cannot be matched with each other. In addition, assumed only two boron species of $B(OH)_4^-$ and $B_4O_5(OH)_4^{2-}$, were used in this system for the calculation, but other boron species may be present in the brine, such as $B(OH)_3$, $B_3O_3(OH)_5^{2-}$, and $B_3O_3(OH)_4^-$ [6, 27]. The results show that this assumption is not precise enough. The relative errors for the experimental solubility calculated using the concentration of lithium and boron are a little larger. It is worth noting that the errors between experimental solubility and computed results are unavoidable. Thus, a large number of thermodynamic models for boron-containing systems are necessary to fit the Pitzer model. The concentration of various boron species can be obtained similarly using the concentration between different boron species [6], pH value, reaction equilibrium constant, etc. [32, 33]. In the calculation of the boron ion, its activity coefficient is considered to be 1.0 [6]. The existing literature shows that the reaction equilibrium constants between different boron species have not been reported in the lithium borate system. For this work, we have chosen an approximation of the reaction equilibrium constant for calculation [6]. Figure 6 shows the boron species' calculated distribution in this quaternary system ($LiCl + LiBO_2 + Li_2B_4O_7 + H_2O$), and the main boron species in the different curves vary greatly. In curves DF_2 and BF_2, the main boron species include $B(OH)_4^-$ and $B_4O_5(OH)_4^{2-}$. Other types of boron can be ignored. In curve F_1F_2, the $B_3O_3(OH)_4^-$ can be ignored. In curve CF_1, $B(OH)_3$ is the main boron species, which may be caused by m(LiCl). Licl solution Is acidic, and as m(LiCl) increases, $B(OH)_3$ is formed by combining $B(OH)_4^-$ and H^+. So, calculations assuming two boron species in solution may not be precise enough. The solubility of lithium borate is the main target of our study rather than the concentration of boron species in this study. Therefore, boron species other than $B(OH)_4^-$ and $B_4O_5(OH)_4^{2-}$ were not considered in this solubility calculation due to the lack of parameters for various boron species at 308.15 K.

5. Conclusion

In this paper, the isothermal solution equilibrium method carried out the phase equilibrium study in the system ($LiCl + LiBO_2 + Li_2B_4O_7 + H_2O$) at 308.15 K. According to each experimental data of the measured equilibrium solution, the corresponding phase diagrams were obtained. The dry-salt diagram of the quaternary system includes two invariant points, four single salt crystallization fields for $LiCl{\cdot}H_2O$, $LiBO_2{\cdot}2H_2O$, $LiBO_2{\cdot}8H_2O$ and $Li_2B_4O_7{\cdot}3H_2O$, and five univariant solubility curves. The densities, refractive indices, and pH values of this system show certain regularity with the increased concentration of lithium metaborate in the solution. In addition, the results calculated by the empirical equation are highly identical to the experimental data. The solubility of this system was calculated based on the Pitzer model combined with the corresponding Pitzer parameters and the solubility product constant of the solid equilibrium phase. There is a certain deviation in the calculated solubility compared with the experimental value in

this system. Although the assumption that there are only two boron species in the brine cannot be fully applied to solubility calculations, the results of such calculations are still able to explain the experimental values well. The phase diagrams and thermodynamic model results in the quaternary system ($LiCl + LiBO_2 + Li_2B_4O_7 + H_2O$) can not only supplement the database of such boron resources but also provide a theoretical basis for their comprehensive utilization and provide a good theoretical reference value for the construction of general thermodynamic models.

Data Availability

The data used to support the findings of this study are available from the corresponding author upon request.

Conflicts of Interest

The authors declare that they have no conflicts of interest.

Acknowledgments

This work was financially supported by the Key Project of Regional Innovation of the National Natural Science Foundation of China (U21A20299), Natural Science Foundation of Shandong Province, China (ZR2020MB051) and Yangtze Scholars and Innovative Research Team of the Chinese University (IRT-17R81).

References

[1] Z. G. Zou, D. S. Zhang, and Z. R. Tan, "Ground brine resource and its exploitation in Shandong province," *Geological Survey and Research*, vol. 31, pp. 214–221, 2008.

[2] P. S. Song, "The phase diagram of salt-water systems and utilization of salt lake resources," *Salt Lake Research*, vol. 24, pp. 35–49, 2016.

[3] Q. S. Fan, Y. Q. Ma, H. D. Cheng et al., "Boron occurrence in halite and boron isotope geochemistry of halite in the Qarhan salt lake, western China," *Sedimentary Geology*, vol. 322, pp. 34–42, 2015.

[4] S. Q. Wang, J. Yang, C. C. Shi, D. Zhao, Y. F. Guo, and T. L. Deng, "Solubilities, densities, and refractive indices in the ternary systems ($LiBO_2 + NaBO_2 + H_2O$) and ($LiBO_2 + KBO_2 + H_2O$) at 298.15 K and 0.1 MPa," *Journal of Chemical and Engineering Data*, vol. 64, no. 7, pp. 3122–3127, 2019.

[5] H. J. Qin, J. T. Wu, S. Q. Wang, Y. F. Guo, and J. Yang, "Solid–Liquid phase equilibria of the reciprocal quaternary system ($Li + Na + Cl + BO_2 + H_2O$) at 288.15 K and 0.1 MPa," *Journal of Chemical and Engineering Data*, vol. 66, no. 1, pp. 761–766, 2020.

[6] H. W. Ge, Y. Fang, C. H. Fang et al., "Density electrical conductivity, pH, and polyborate distribution of $LiB(OH)_4$, $Li_2B_4O_5(OH)_4$, and $LiB_5O_6(OH)_4$ solutions," *Journal of Chemical and Engineering Data*, vol. 59, no. 12, pp. 4039–4048, 2014.

[7] L. Yang, X. X. Yang, D. Li et al., "Solubility measurement and thermodynamic modeling of solid-liquid equilibria in quaternary system $NaCl - Na_2SO_4 - NaBO_2 - H_2O$ at 323.15 K," *The Journal of Chemical Thermodynamics*, vol. 159, pp. 106472–111072, 2021.

[8] J. J. Yu, M. P. Zheng, and Q. Wu, "Research progress of lithium extraction process in lithium-containing salt lake," *Chemical Industry and Engineering Progress*, vol. 32, pp. 13–21, 2013.

[9] W. Y. Zhang, X. P. Li, L. Yang, and S. H. Sang, "Experimental study on phase equilibria in $Na_2B_4O_7 + Na_2SO_4 + H_2O$ and $Li_2B_4O_7 + Na_2B_4O_7 + H_2O$ aqueous ternary systems at 273 K," *Russian Journal of Physical Chemistry A*, vol. 93, no. 6, pp. 1032–1037, 2019.

[10] F. Yuan, H. Li, L. Li, Y. F. Guo, S. Q. Wang, and T. L. Deng, "Solid–Liquid phase equilibria of the ternary system ($KBO_2 + K_2SO_4 + H_2O$) at 288.15, 308.15 K, and 0.1 Mpa," *Journal of Chemical and Engineering Data*, vol. 66, no. 4, pp. 1703–1708, 2021.

[11] X. X. Yang, L. L. Chen, Y. F. Guo, D. Li, T. L. Deng, and L. Z. Meng, "Solid–Liquid phase equilibria of the quaternary system $Li_2SO_4 - LiBO_2 - Li_2B_4O_7 - H_2O$ and the ternary subsystem $LiBO_2 - Li_2B_4O_7 - H_2O$ at $T = 288.15$ K and $p = 0.1$ MPa," *Journal of Chemical and Engineering Data*, vol. 66, pp. 3463–3472, 2021.

[12] X. D. Yu, Y. Zeng, P. J. Chen, and L. G. Li, "Solid-Liquid equilibrium of the quaternary system lithium, potassium, rubidium, and borate at $T = 323$ K," *Journal of Chemical and Engineering Data*, vol. 63, no. 8, pp. 3125–3129, 2018.

[13] F. Yuan, L. Li, Y. F. Guo, M. L. Li, J. Duo, and T. Deng, "Solubilities, densities and refractive indices for the two ternary systems ($Li_2SO_4 + LiB_5O_8 + H_2O$) and ($LiCl + LiB_5O_8 + H_2O$) at 298.15 K and 101.325 kPa," *Journal of Solution Chemistry*, vol. 49, no. 11, pp. 1430–1441, 2020.

[14] X. D. Yu, M. P. Zheng, Y. Zeng, and L. Wang, "Solid–Liquid equilibrium of quinary Aqueous solution composed of lithium, potassium, rubidium, magnesium, and borate at 323.15 K," *Journal of Chemical and Engineering Data*, vol. 64, no. 12, pp. 5681–5687, 2019.

[15] D. L. Gao, Y. F. Guo, X. P. Yu, S. Q. Wang, and T. L. Deng, "Solubilities, densities, and refractive indices in the Salt-Water ternary system ($LiCl + LiBO_2 + H_2O$) at $T = 288.15$ and 298.15 K and $p = 0.1$ MPa," *Journal of Chemical and Engineering Data*, vol. 60, no. 9, pp. 2594–2599, 2015.

[16] N. Zhang, Y. F. Guo, Y. Yuan, S. Q. Wang, and T. L. Deng, "Thermodynamic phase equilibria of the aqueous ternary system ($LiCl + LiBO_2 + H_2O$) at 308 K: experimental data and predictions using the pitzer model," *Journal of Chemical Engineering of Japan*, vol. 49, no. 4, pp. 324–331, 2016.

[17] L. Li, Y. F. Guo, S. S. Zhang, M. M. Shen, and T. L. Deng, "Phase equilibria in the aqueous ternary systems ($LiCl + LiBO_2 + H_2O$) and ($Li_2SO_4 + LiBO_2 + H_2O$) at 323.15 K and 0.1 MPa," *Fluid Phase Equilibria*, vol. 436, pp. 13–19, 2017.

[18] L. Yang, L. L. Chen, T. Zhang et al., "Solubility determination and thermodynamic modeling of solid–liquid equilibria in the $LiBO_2 - Li_2B_4O_7 - H_2O$ system at 298.15 K and 323.15 K," *Fluid Phase Equilibria*, vol. 523, Article ID 112783, 2020.

[19] D. Li, Q. T. Fu, T. Zhang et al., "Thermodynamic modeling of boron species in brine systems containing metaborate and its application in evaporation simulation," *Journal of Materials Research and Technology*, vol. 9, no. 6, pp. 13067–13075, 2020.

[20] D. Li, L. Z. Meng, Y. F. Guo, T. L. Deng, and L. Yang, "Chemical engineering process simulation of brines using phase diagram and pitzer model of the system $CaCl_2 - SrCl_2 - H_2O$," *Fluid Phase Equilibria*, vol. 484, pp. 232–238, 2019.

[21] S. Q. Chen, W. J. Cui, J. Y. Hu, Y. F. Guo, and T. L. Deng, "Phase equilibria and phase diagrams for the aqueous ternary system containing sodium, sulfate, and metaborate Ions at

288.15 and 308.15 K and 101.325 kPa," *Journal of Chemical and Engineering Data*, vol. 64, no. 6, pp. 2809–2815, 2019.

[22] Qinghai Institute of Salt Lakes Chinese Academy of Sciences, *Analytical Methods of Brines and Salts*, China Science Press, Beijing, China, 2nd edition, 1988.

[23] P. S. Song, X. H. Du, and H. C. Xu, "Studies on the phase equilibrium and physicochemical properties of the ternary system $Li_2B_4O_7 - Li_2SO_4 - H_2O$ at 25°C," *Chinese Science Bulletin*, vol. 28, pp. 106–110, 1983.

[24] L. Z. Meng, M. S. Gruszkiewicz, T. L. Deng, Y. F. Guo, and D. Li, "Isothermal evaporation process simulation using Pitzer model for the quinary system $LiCl - NaCl - KCl - SrCl_2 - H_2O$ at 298.15 K," *Industrial and Engineering Chemistry Research*, vol. 54, no. 33, pp. 8311–8318, 2015.

[25] H. T. Kim and W. J. Frederick, "Evaluation of Pitzer ion interaction parameters of aqueous electrolytes at 25 degree. C. 1. Single salt parameters," *Journal of Chemical and Engineering Data*, vol. 33, no. 2, pp. 177–184, 1988.

[26] K. S. Pitzer, *Activity Coefficients in Electrolyte Solutions*, CRC, Boca Raton, FL, USA, 1991.

[27] T. Zhang, D. Li, and L. Z. Meng, "Recent progresses on the boron species in aqueous solution: structure, phase equilibria, metastable zone width (MZW) and thermodynamic model," *Reviews in Inorganic Chemistry*, vol. 41, no. 1, pp. 49–60, 2021.

[28] X. C. Ma, Y. Yao, and R. L. Wang, "Studies of the activity coefficients of LiCl for $LiCl - Li_2SO_4 - H_2O$ system at 0, 15, 35°C by Emf method," *Journal of Salt Lake Research*, vol. 3, pp. 45–51, 1995.

[29] T. L. Deng, "Phase equilibrium for the aqueous system containing lithium, sodium, potassium, chloride, and borate ions at 298.15 K," *Journal of Chemical and Engineering Data*, vol. 49, no. 5, pp. 1295–1299, 2004.

[30] H. C. Li, *Study on Stable Phase Diagram of Old Brine Containing Lithium Quinary System In West Taijinar Brine at 308 K*, Chengdu University of Technology, Chengdu, China, 2017.

[31] X. X. Yang, S. S. Gu, Y. F. Guo, T. L. Deng, D. Li, and L. Z. Meng, "Solubility determination and thermodynamic modeling in the quaternary system $Li_2SO_4 - LiBO_2 - Li_2B_4O_7 - H_2O$ at $T = 308.15$ K and $p = 0.1$ MPa," *The Journal of Chemical Thermodynamics*, vol. 168, Article ID 106729, 2022.

[32] J. E. Spessard, "Investigations of borate equilibria in neutral salt solutions," *Journal of Inorganic and Nuclear Chemistry*, vol. 32, no. 8, pp. 2607–2613, 1970.

[33] R. E. Mesmer, C. F. Baes, and F. H. Sweeton, "Acidity measurements at elevated temperatures. VI. Boric acid equilibriums," *Inorganic Chemistry*, vol. 11, no. 3, pp. 537–543, 1972.